A&A manuscript no.
(will be inserted by hand later)

Your thesaurus codes are:
06(08.06.2; 08.12.1; 08.16.5; 13.25.5; 04.19.1)

ASTRONOMY
AND
ASTROPHYSICS
16.10.1996

New 'weak-line'–T Tauri stars in Lupus * **

J. Krautter[1], R. Wichmann[1], J.H.M.M. Schmitt[2], J.M. Alcalá[2,4], R. Neuhäuser[2], and L. Terranegra[3]

[1] Landessternwarte Königstuhl, D-69117 Heidelberg, Germany
[2] Max-Planck-Institut für Extraterrestrische Physik, D-85740 Garching, Germany
[3] Osservatorio Astronomico di Capodimonte, Via Moiariello 16, I-80131 Napoli, Italy
[4] Instituto Nacional de Astrofísica Optica y Electrónica, A.P. 51 y 216, CP 72000, Puebla, México

Received ; accepted

Abstract. We present first results obtained by a survey of the Lupus star forming region in search of new T Tauri stars. This study has been performed on the basis of deep pointed ROSAT observations in the Lupus dark clouds as well as data from the ROSAT All-Sky-Survey in the surrounding, less obscured regions. Our survey covers an area of about 230 square degrees, located between $15^h\,6^m$ and $16^h\,24^m$ in right ascension and between -47^o and -32^o in declination. Identification of ROSAT All-Sky-Survey sources in this area by means of optical spectroscopy revealed 89 T Tauri stars, 86 of them 'weak-line' T Tauri stars (WTTS) not known from previous studies of this region. Our pointed ROSAT observations led to the identification of 47 more T Tauri stars, giving a total of 136 new T Tauri stars. The large area of our study, as compared with previous works, allows us to study the spatial distribution of WTTS in this star forming region on a large scale. We find the new WTTS to be distributed over the whole area of our survey, indicating that their spatial distribution might extend well beyond our study area. Contrary to the Lupus T Tauri stars known prior to this study, the WTTS discovered by the ROSAT All-Sky-Survey are not clustered in the regions of highest extinction, i.e. the dark clouds.

Key words: Stars: formation – Stars: late-type – Stars: pre-main sequence – X-rays: stars – Surveys

1. Introduction

The study of T Tauri stars (TTS), first recognized by Ambartsumian (1947) as low-mass pre-main sequence stars, provides insights into the process of star formation and the evolution of stars towards the main sequence. Important issues currently investigated are the frequency of binaries and the distribution of their separations (Leinert et al. 1993, Ghez et al. 1993), which may yield constraints on the models of star formation, as well as the evolution of the angular momentum of TTS (Bouvier et al. 1993a, 1993b).

Another important aspect is the fact that even in well-known star forming regions (SFR) the true number of TTS is quite uncertain, leading to uncertainties in the derivation of the initial mass function (IMF) as well as in the estimates of the efficiency of the star forming process. Moreover, as pointed out by Herbig (1978) there should exist a numerous population of so-called post-T Tauri-stars (PTTS), i.e. TTS that have evolved from the population of classical TTS (CTTS) towards the main sequence and therefore should show properties very similar to normal main-sequence stars. As compared to the large expected numbers of PTTS, only few stars that might belong to this population have been identified so far, while many of the known WTTS are more or less coeval with the CTTS.

WTTS often show strong X-ray emission, and therefore are most easily detected in the X-ray band, while due to their lack of strong emission lines in the optical spectral range most of these stars are very difficult to detect by optical objective prisms surveys like those carried out in Lupus by Schwartz (1977) and Thé (1962).

In a previous paper (Wichmann et al. 1996a) we have presented results obtained from a similar survey of the Taurus-Auriga SFR based on the ROSAT All-Sky-Survey (RASS). Here we present first results from a similar study of the Lupus SFR. At a distance of 140 pc (Hughes et al. 1993), Lupus belongs to the nearest nearby star forming regions. Its population of 60 T Tauri-stars known prior to ROSAT (Krautter 1991) is concentrated in four small subgroups (Lupus 1–4). The mass spectrum of these TTS

Send offprint requests to: J. Krautter

* Based on observations collected at European Southern Observatory, La Silla, Chile (observing proposals ESO No. 49.7-0010, 50.7-0109, 51.7-0106, 51.7-0029).

** Tables 5 – 12 are only available in electronic form at the CDS via anonymous ftp 130.79.128.5.

was found to be quite unusual, as it exhibits a higher proportion of very low-mass stars than found in other SFRs (Hughes et al. 1994). The area of our study covers about 230 square degrees and is located between $15^h\,6^m$ and $16^h\,24^m$ in right ascention and between -47^o and -32^o in declination, thus not only covering all four subgroups, but extending significantly beyond them.

2. Candidate stars from the ROSAT All-Sky Survey

The All-Sky Survey performed by the German X-ray satellite ROSAT offers for the first time the opportunity to study a spatially complete sample of X-ray sources in any star forming region. For a detailed description of ROSAT and its detectors we refer to Trümper (1983) and Pfeffermann et al. (1986). During the RASS the sky was scanned in great circles, using the Positional Sensitive Proportional Counter (PSPC). Each object in the sky was observed during several scans once every 93 minutes for up to about 30 sec per scan. The number of scans per object depends on the ecliptic latitude. In the Lupus area each point in the sky was observed during some 30 scans, giving a mean exposure time of 406 sec with an rms scatter of 42 sec.

The RASS data were reduced using the EXSAS (EXtended Scientific Analysis System) software package developed at MPE, Garching. Source detection was performed seperately in five different energy bands – broad (0.1-2.4 keV), soft (0.1-0.4 keV), hard (0.5-2.4 keV), hard1 (0.5-0.9 keV) and hard2 (0.9-2.4 keV). After application of both local and map source detection algorithms detected sources were merged and tested with a maximum likelihood technique (Cruddace et al. 1988). We used a treshold of $ML \geq 8$ for the likelihood of existence ML, which is defined as $ML = -\ln(1-P)$ (where P is the probability for the existence of a source). This procedure resulted in the detection of 437 sources.

For the selection of candidate sources we first searched the SIMBAD database for optical counterparts of the X-ray sources. We excluded all sources that could be identified with known objects within 60" from the X-ray position. (The positional accuracy of the RASS is discussed, e.g., by Motch et al. 1991 and Neuhäuser et al. 1995b. We decided to use a rather conservative, i.e. large error circle.)

Catalogued stars, for which a TTS nature could neither be ascertained nor rejected on the basis of available data, were kept in the list for further study. Next we visually inspected the ESO SRC(R) plates to exclude all sources without a stellar object of $m_R \lesssim 15$ (which converts to $m_V \lesssim 16$ for an M2 V star) inside the aforementioned error radius. This resulted in a final list of 298 candidate sources for spectroscopic follow-up observations. Unlike in our study of the Taurus SFR (Wichmann et al. 1996a), no selection of candidate objects by means of the X-ray energy distribution has been performed.

Table 1. Pointed observations in Lupus 1

α (2000)	δ (2000)	Exposure time [sec]	Date
15 39 26	-34 07 12	3054	26.08.92
15 39 26	-34 27 00	1344	01.03.91
15 39 26	-34 46 48	1764	29.02.92
15 41 02	-34 07 12	2082	28.08.92
15 41 04	-34 27 00	1132	27.02.93
15 41 04	-34 46 48	996	26.02.92
15 41 05	-34 46 48	1693	29.08.93
15 42 41	-34 07 12	1085	26.02.93
15 42 41	-34 46 48	842	27.02.93
15 44 17	-34 07 12	969	25.02.93
15 44 17	-34 07 12	1703	30.08.93
15 44 17	-34 27 00	877	26.02.93
15 44 17	-34 27 00	1302	06.03.93
15 44 19	-34 46 48	980	27.02.93
15 44 19	-34 46 48	1209	11.08.93
15 45 55	-34 07 12	783	26.02.93
15 45 55	-34 07 12	636	05.09.93
15 45 55	-34 27 00	972	06.03.92
15 45 55	-34 27 00	698	07.03.92
15 45 55	-34 46 48	1829	28.02.93
15 46 19	-35 13 48	1651	06.03.92
15 46 17	-35 34 12	968	28.02.93
15 46 17	-35 34 12	775	01.03.93
15 46 17	-35 34 12	1002	14.08.93
15 46 17	-35 54 00	1312	03.03.93
15 47 58	-34 49 12	1043	01.03.93
15 47 58	-34 49 12	974	13.08.93
15 47 58	-35 13 48	1235	04.03.93
15 47 58	-35 34 12	1111	02.03.93
15 47 58	-35 54 00	787	02.03.93
15 47 58	-35 54 00	672	30.08.93
15 49 36	-35 13 48	930	27.02.93
15 49 36	-35 34 12	1510	08.03.92
15 49 36	-35 54 00	1407	04.03.93
15 51 12	-35 34 12	1724	08.03.92
15 51 14	-35 54 00	1198	04.03.93
15 51 14	-36 13 48	1049	04.03.93

3. Pointed ROSAT observations

In addition to the RASS, we performed a raster scan of pointed ROSAT observations covering the Lupus 1–3 subgroups. The journal of these pointed observations is given in Tables 1, 2, and 3. The reduction of these data was performed using EXSAS. The first step consisted in merging the photon event tables (PETs) of the individual observations, containing the data for each registered X-ray photon during the observation, into one single PET for each of the three observed Lupus subgroups. Then on each of these three PETs, like for the RASS data, source detection was performed seperately in the five different energy bands mentioned above. After application of both local and map

Table 2. Pointed observations in Lupus 2

α (2000)	δ (2000)	Exposure time [sec]	Date
15 53 31	-37 31 12	871	09.03.92
15 53 31	-37 31 12	1277	04.03.93
15 53 29	-37 51 00	1381	04.03.93
15 53 29	-37 51 00	1396	10.03.92
15 53 31	-38 11 24	2307	09.03.92
15 55 12	-37 31 12	1175	09.03.91
15 55 10	-37 51 00	734	09.03.92
15 55 10	-37 51 00	793	10.03.92
15 55 10	-38 11 24	2146	09.03.92
15 56 53	-37 31 12	2264	09.03.92
15 56 53	-37 51 00	1816	09.03.92
15 56 53	-38 11 24	1259	09.03.91
15 58 34	-37 31 12	1286	09.03.91
15 58 34	-37 51 00	1213	08.03.91
15 58 34	-38 11 24	1241	09.03.91

Table 3. Pointed observations in Lupus 3

α (2000)	δ (2000)	Exposure time [sec]	Date
16 05 24	-38 46 12	1317	06.03.93
16 05 24	-39 06 00	1386	07.03.93
16 05 24	-39 25 48	1794	11.03.92
16 05 24	-39 46 12	1061	11.03.91
16 07 07	-38 46 12	1426	07.03.93
16 07 07	-39 06 00	1509	07.03.93
16 07 07	-39 25 48	1383	07.03.93
16 07 07	-39 46 12	1383	07.03.93
16 07 05	-40 06 00	899	11.03.91
16 07 05	-40 06 00	647	07.03.93
16 07 05	-40 06 00	1400	07.03.93
16 07 05	-40 06 00	1208	04.09.93
16 08 50	-38 46 12	1318	10.03.91
16 08 50	-39 06 00	1478	10.03.91
16 08 50	-39 25 48	1389	10.03.91
16 08 50	-39 46 12	1359	11.03.91
16 08 50	-40 06 00	1472	08.03.93
16 10 34	-38 46 12	1423	11.03.91
16 10 34	-39 06 00	823	08.03.93
16 10 34	-39 06 00	1051	28.08.93
16 10 34	-39 06 00	985	04.09.93
16 10 34	-39 25 48	1340	12.03.92
16 10 36	-39 46 12	1892	12.03.92
16 10 36	-40 06 00	1429	13.03.91
16 12 17	-38 46 12	1214	12.03.92
16 12 17	-38 46 12	1385	07.03.93
16 12 17	-39 06 00	766	10.03.92
16 12 17	-39 06 00	705	12.03.92
16 12 17	-39 06 00	1511	08.03.93
16 12 17	-39 25 48	1676	13.03.91
16 12 19	-39 46 12	1060	13.03.91
16 12 19	-40 06 00	1740	11.03.92

source detection algorithms, detected sources were merged and tested with a maximum likelihood technique (Cruddace et al. 1988).

In a pointed ROSAT observation the size of the point spread function increases from the center of the field of view outwards, while in the survey it retains a constant value, thus demanding somewhat different settings of the parameters of the source detection algorithms (the main difference being the size of the sliding window). As our raster scan did not conform to either of these two cases, we tried a variety of parameter settings, judging the results by visual inspection of the X-ray images. We obtained the best results for a combination of the window size for pointed observations, a constant value for the FWHM of the point spread function (60 arcsec) in the maximum-likelihood test, and a conservative value of $ML \geq 10$.

This procedure yielded 70 X-ray sources in Lupus 1, 52 sources in Lupus 2 and 96 sources in Lupus 3. To these sources the same selection procedure was applied as to the RASS sources. I.e. we excluded sources with a counterpart of known nature in the SIMBAD database and selected candidate sources for optical follow-up observations, according to the same criteria as mentioned above for the RASS source list.

4. Spectroscopic observations

Spectroscopic follow-up observations for identification of stellar counterparts have been performed at European Southern Observatory, Chile, during five observing runs. In the first run (09.05.91–19.05.91) we used the MPIA 2.2 m-telescope with the Boller & Chivens spectrograph, the RCA HR CCD and grating ♯16, which gave a resolution of 7.9 Å and a spectral range of 4800–6800 Å. In the four following runs (03.05.92–12.05.92, 26.03.93–02.04.93, 29.05.93–06.06.93, and 28.06.93–04.07.93) we observed at the ESO 1.52 m-telescope with the B&C spectrograph, the FA2K CCD (ESO ♯27) and grating ♯5. The resolution was 4.5 Å and the spectral range 4500–6800 Å. (The resolution was measured from unblended lines of the He-Ar calibration lamp.) For each star a He-Ar wavelength calibration frame was obtained at the respective position. Three spectrophotometric standard stars were observed each night, and spectral standards were established by observing stars with spectral types ranging from G0 to M4 from the MK star catalog (Buscombe 1981, 1988).

Data reduction was performed using MIDAS (Munich Image and Data Analysis System). The reduction consisted of bias subtraction, division by a flatfield, wavelength calibration, sky subtraction, extraction of the one-dimensional spectrum and flux calibration. As the weather was usually not photometric, only relative flux calibration could be achieved.

Spectral classification was accomplished by comparison with the spectral standards from the MK catalog following the procedure outlined in Wichmann et al. (1996a).

5. Optical counterparts

We investigated a total of 156 RASS sources and an additional number of 79 sources from pointed observations. On average, there were about two candidate counterparts per source. With regard to the discussion of candidate selection on the basis of X-ray hardness ratios below, we stress, that all the investigated sources have been selected at random from the input source lists, regardless of their hardness ratios or X-ray luminosity.

5.1. The T Tauri-stars

A star was classified as TTS if it showed a late spectral type (F or later), and a Li I $\lambda6707$ absorption line with an equivalent width W_λ of $W_\lambda \geq 100\,m\AA$.

Stars classified as TTS were subdivided in WTTS and CTTS on the basis of their Hα emission. If Hα was present in emission above the photospheric continuum with an equivalent width $W_{H\alpha}$ in excess of 10Å, the star was classified as CTTS, otherwise as WTTS. However, we did not use the presence of Hα emission as indicator for the pre-main sequence nature of a star, because some late-type main sequence stars have significant Hα emission, while in some PMS stars the Hα emission may not even fill up the photospheric absorption.

Of 156 RASS sources studied so far, 86 have been identified with TTS. In three cases two TTS were found within the error circle, thus the total number of TTS found on the basis of the RASS is 89 (86 WTTS and 3 CTTS). Additionaly, out of 92 sources of pointed observations we studied, 46 could be identified with TTS. In one case two TTS were found within the error circle, thus 47 additional TTS (45 WTTS and 2 CTTS) were found on the basis of the pointed observations.

The new WTTS found in our study are listed in Table 5. If possible, stars are named by a catalog identifier, otherwise the RASS source name is given. Whenever possible, the coordinates are taken from the Hubble Guide Star Catalog (GSC).

5.2. Other emission-line objects

During our survey, 44 stars of spectral type K to M were found, which displayed Hα in emission above the continuum, but most probably are not PMS stars, as none of them shows obvious Li I $\lambda6707$ absorption. These stars are listed in Table 6. As we do not have photometric data for these stars, we cannot make any statement concerning their distance or a possible association with the Lupus SFR. The number of these stars is within the expected range, as a comparison with the EINSTEIN Medium Sensitivity Survey (EMSS; Stocke et al. 1991) shows. The EMSS has a limiting sensitivity ranging from $\sim 5 \times 10^{-14}$ to $\sim 3 \times 10^{-12}$erg cm^{-2} s^{-1}, which is comparable to the sensitivity of the RASS. 26% of the EMSS sources were identified with galactic stars, most of them active late-type dwarfs.

5.3. Special objects

5.3.1. RXJ1556.1-3655

We identified this source with a CTTS with strong Hα emission ($W_\lambda = 76\,\AA$) and marked emission in Hβ, He I $\lambda\lambda5875$, 6678, and [O I] $\lambda6300$. This star is identical with Thé 11 (Thé 1962). Although the star is only about 1.1^o from the center of plate CS 19279 of the objective prism survey carried out by Schwarz (1977), it is not listed in the paper, and apparently has never been studied in more detail. This star may exhibit strong variability in the Hα line, which could be the reason why it has not been found by Schwarz (1977).

5.3.2. RXJ1544.0-4447

In the error circle of this source we found a star of spectral type M4 with a rather strong Hα emission ($W_\lambda = 30\,\AA$). Also Hβ and He I $\lambda5865$ are in emission. However, although the Hα emission is much stronger than usually found for dMe-stars, no Li I $\lambda6708$ absorption could be found. As the absorption spectrum of this star is relatively weak in comparison with other stars of the same spectral type, we suspect that the Li I line might be hidden by veiling and tentatively identify this object as CTTS candidate.

6. Completeness of the survey

If we want to estimate the completeness of the discovered TTS population of TTS in Lupus, we have to take into account first, that not all TTS within the region of interest are detected by ROSAT as X-ray sources, and second, that not all of the detected X-ray sources in the region of interest have been spectroscopically studied as yet.

6.1. Completeness with regard to X-ray detection

Although spatially complete, the RASS is flux limited. Therefore, in order to estimate the fraction of TTS that escaped detection, ideally we have to compare the X-ray luminosity function (XLF) of the RASS-discovered WTTS with an unbiased XLF of WTTS, thus determining which fraction of this unbiased XLF is sampled by the RASS in Lupus.

For the construction of the XLF of the newly discovered WTTS we followed the procedure described in detail in previous papers (Neuhäuser et al. 1995b, Wichmann et al. 1996a). We calculate luminosities L_X for our new WTTS as

$$L_X = 4\pi r^2 (ECF)^{-1} Z, \tag{1}$$

where Z is the broadband count rate, r the distance to the Lupus SFR, taken to be 140 pc (Hughes et al., 1993), while ECF denotes the energy conversion factor. ECF was calculated individually for each TTS of our sample by fitting Raymond-Smith spectra (Raymond & Smith 1977) to the observed X-ray hardness ratios in the way described in Neuhäuser et al. (1995b).

Since photometry is available for many of our new WTTS (Wichmann et al. 1996b), we were able to calculate A_V for these stars, thus in these cases the only free parameter for the fit was T_X. For stars with no known A_V, fit were done with two free parameters (temperature T_X, and hydrogen column density N_H). The X-ray data for all ROSAT-discovered TTS are given in Table 10, the fit results for the X-ray luminosity in Table 11, respectively.

X-ray luminosities for TTS known prior to ROSAT are given in Table 12, as obtained from the pointed observations listed in Table 1 to 3, with N_H calculated from published values of the visual extinction A_V (Hughes et al. 1994).

For the conversion from A_V to N_H we used the relation

$$\frac{N_H}{cm^2} = 5.5 \cdot 10^{21} \frac{E_{B-V}}{mag} = \frac{5.5}{3.1} \cdot 10^{21} \frac{A_V}{mag}, \tag{2}$$

following the detailed investigation of absorption in the local environment and of TTS by Paresce (1984) and Vrba & Rydgren (1985).

The best available estimate of an unbiased XLF of WTTS is presumably given by the XLF of WTTS that originally were optically discovered, i.e. by means of H_α or Ca HK surveys or by proper motion surveys. A large sample of such WTTS in the Taurus-Auriga star forming region has recently been studied by Neuhäuser et al. 1995b.

As found by Neuhäuser et al. (1995b), the mean X-ray luminosity of CTTS is significantly lower than that of WTTS. A large fraction of the previously known (i.e. optically discovered) CTTS in Lupus have been observed in our pointed ROSAT observations (see Table 12). We obtain a mean X-ray luminosity of $\log(L_X[erg/s]) = 29.00 \pm 0.03$ for the Lupus CTTS, significantly below the mean X-ray luminosity of $\log(L_X[erg/s]) = 29.66 \pm 0.05$ determined by Neuhäuser et al. 1995b for the (optically discovered) Taurus WTTS (the number of previously known WTTS in Lupus is too low for a meaningful comparison with CTTS). This result agrees well with that of Neuhäuser et al. (1995b), who found for Taurus that the CTTS are significantly less X-ray luminous than the WTTS. We conclude that the (absorption corrected) mean X-ray luminosity of CTTS is intrinsically lower than that of the WTTS.

In Fig.1 we show the XLF of RASS-discovered WTTS (without WTTS discovered in pointed observations) in comparison with the XLFs of previosly known Lupus CTTS and optically discovered Taurus WTTS, respectively. Also shown is the XLF of new WTTS discovered by pointed observations in Lupus 1-3. The derived mean and median luminosities for these four samples are given in Table 4.

From Fig.1 as well as from the data given in Table 4 we see that the mean X-ray luminosity of RASS-discovered WTTS is much higher than that one of the optically discovered Taurus WTTS, due to the bias introduced by the flux limit of the RASS. On the other hand, the XLF of the WTTS discovered by means of pointed observations in the Lupus 1-3 clouds is indistiguishable from that of the optically discovered Taurus WTTS. Thus in the Lupus 1-3 clouds, with our deep pointed observations presumably nearly all WTTS are detected as X-ray sources.

The XLF of our new WTTS has a value of 0.80 ± 0.04 for $\log(L_X/erg\,s^{-1}) \leq 29.95$, i.e. $80 \pm 4\%$ of our new WTTS show an X-ray luminosity as large or larger than this value.

However, only $25 \pm 7\%$ of WTTS in the unbiased comparison sample have $\log(L_X/erg\,s^{-1}) \geq 29.95$, i.e. an X-ray unbiased sample is complete only to $25 \pm 7\%$ for an X-ray luminosity, which is exceeded by about 80% of our RASS-detected sample of new WTTS. We estimate therefore, that the fraction of previously unknown WTTS, which are sampled by the RASS in Lupus, is $25/80 = 0.31(\pm 0.09)$. (We use the particular value of $\log(L_X/erg\,s^{-1}) \leq 29.95$, because it lies well within the both XLFs of the new WTTS and our comparison sample).

Here we assume, that the WTTS outside the clouds have an XLF similar to WTTS found in the regions of active star formation, like the Lupus clouds or those regions in Taurus-Auriga where WTTS have been found by optical surveys. If, however, the RASS-discovered WTTS are typically older than those of the comparison sample, as might be indicated by their spatial position far from dense clouds, then from theoretical grounds (e.g. Bouvier et al. 1996) their mean X-ray luminosity might be different. Recent models suggest, that only after dissipation of circumstellar material TTS will spin up and their activity could rise accordingly. This might also be the explanation for the generally higher X-ray luminosity of WTTS as compared with CTTS. If this holds true, it would reduce the bias introduced by X-ray selection. However, up to now little is known about the importance of other factors like, e.g., the depth of the convection zone, which decreases during the PMS evolution. Thus, it is not clear how the evolution of the XLF during the PMS phase really looks like.

6.2. Completeness with regard to follow-up observations

Next, we discuss the incompleteness of our optical follow-up observations, i.e. we estimate, what fraction of the

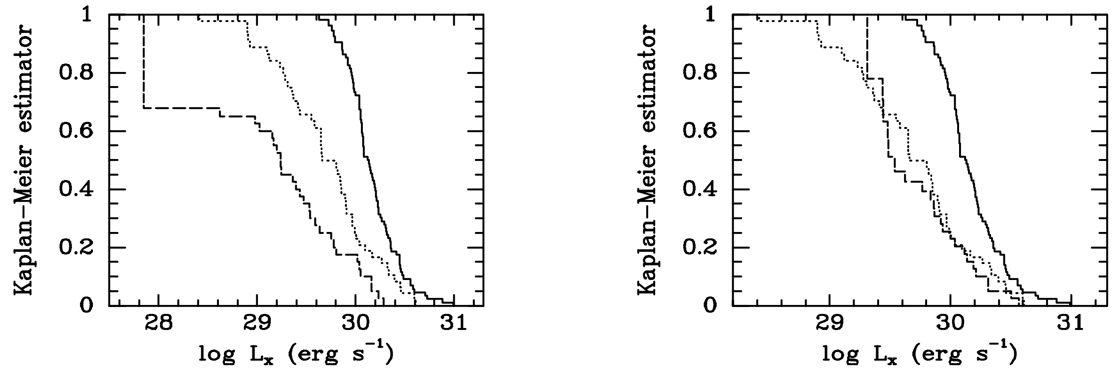

Fig. 1. X-ray luminosity functions of RASS-discovered WTTS (solid line) and WTTS discovered by pointed ROSAT observations (dotted line) in Lupus, as compared with x-ray luminosity functions of Lupus CTTS (left panel, broken line) and optically discovered Taurus WTTS (right panel, broken line). Data for Taurus WTTS were taken from Neuhäuser et al. (1995b).

Table 4. X-ray luminosities of new Lupus WTTS (a: RASS-discovered, b: discovered by pointed observations), Lupus CTTS in the Lupus 1-3 clouds, and (for comparison) Taurus WTTS. Data for Taurus WTTS from Neuhäuser et al. 1995b. Due to the large number of upper limits, no reliable estimate for $\log(L_X)^{1st\,quartile}$ is possible for the Lupus CTTS.

Sample	Size	$\log(L_X)^{mean}$	$\log(L_X)^{1st\,quartile}$	$\log(L_X)^{median}$	$\log(L_X)^{3rd\,quartile}$
Taurus WTTS	34	29.66±0.05	27.96	29.52	29.94
Lupus WTTS (a)	85	30.16±0.03	29.98	30.12	30.31
Lupus WTTS (b)	48	29.69±0.07	29.31	29.66	29.99
Lupus CTTS	40	29.00±0.14	-	29.24	29.64

WTTS detected as X-ray sources in the RASS have been identified by our survey already and how much WTTS are to be expected among those sources not observed as yet. Based on the RASS data on Taurus TTS, Neuhäuser et al. (1995a) found a selection criterium for WTTS based on the X-ray hardness ratios HR1 and HR2, defined as defined as

$$\mathrm{HR\,1} = \frac{C_B - C_A}{C_B + C_A} \qquad \text{and} \qquad \mathrm{HR\,2} = \frac{C_D - C_C}{C_D + C_C}, \tag{3}$$

where C_A, C_B, C_C, and C_D denote the count rates in the energy bands 0.1 to 0.4 keV, 0.5 to 2.1 keV, 0.5 to 0.9 keV and 0.9 to 2.1 keV, respectively.

86% of all Taurus WTTS known prior to ROSAT, as well as 78% of all WTTS discovered in Taurus by follow-up observations of RASS sources fall in the region defined by

$$-0.15 \leq HR1 \leq 1 \qquad \text{and} \qquad -0.3 \leq HR2 \leq 0.5. \tag{4}$$

in the HR1–HR2 plane. As no selection based on hardness ratios has been used for our follow-up observations of ROSAT sources in Lupus, we can test this criterium *a posteriori* with our new Lupus WTTS. As can be seen from Fig. 2, in fact the majority of our new WTTS occupy the region given by Eq. 4. Of 126 sources identified with WTTS, 74% are found inside this box, while the percentage of WTTS among those investigated sources located within the selection box is 67%.

Of 437 X-ray sources in the RASS, 238 are situated within the region given by Eq. 4. 105 of those are TTS or other sources of known nature, while 133 are sources of unknown nature. From the results quoted above, we would expect about 67% of the latter, i.e., 89 sources, to be WTTS. Moreover, these 89 WTTS should represent about 74% of all hitherto unidentified WTTS in the RASS, regardless of their hardness ratios. Thus we would expect some 120 WTTS in the RASS not yet identified.

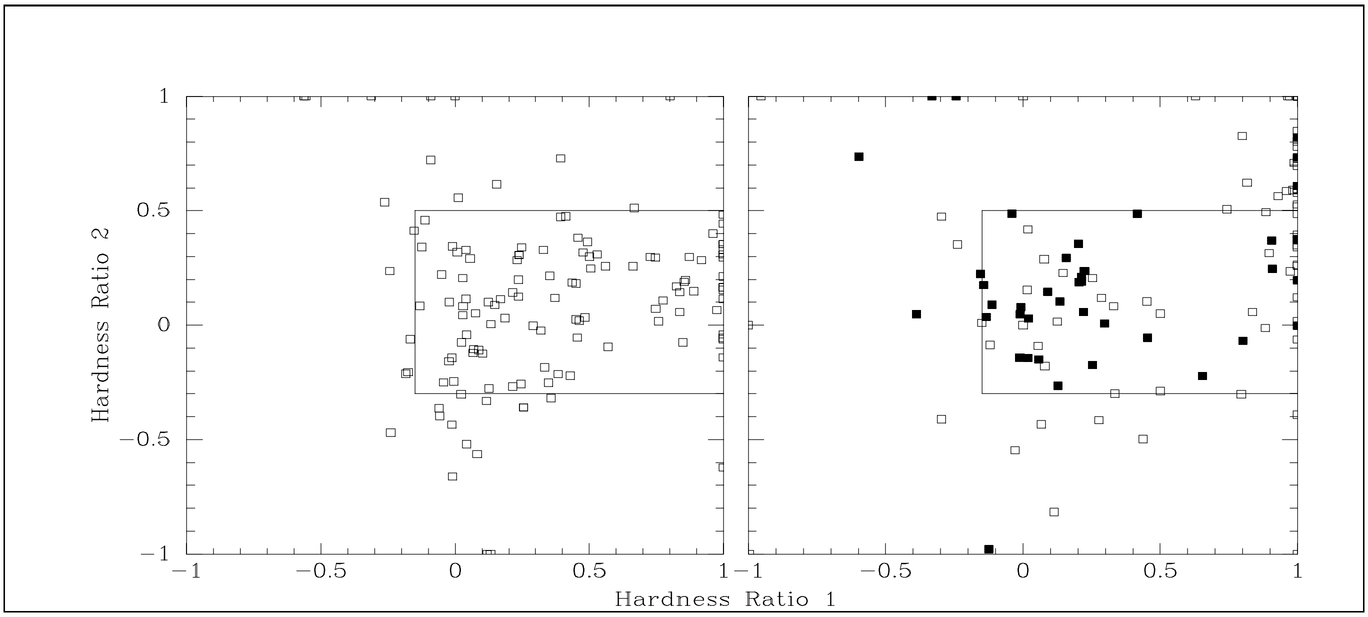

Fig. 2. Hardness ratios for RASS-discovered WTTS in Lupus (left panel) as compared with hardness ratios of sources where no TTS could be found (right panel, solid squares indicate stars dMe/dKe stars, open squares other/no identification). The lines mark the box defined by Neuhäuser et al. (1995a) for selection of TTS candidates.

However, in our survey we have restricted ourselves to sources where at least one stellar object brighter than $m_R \simeq 15$ can be found within the error circle. Thus, the fractions of sources inside/outside the HR box only pertain to that subsample of sources which fullfill this optical selection criterium. Also the number of 120 more WTTS should be regarded as an upper limit for WTTS *brighter than* $m_R \simeq 15$, as at least some of the sources not yet investigated will not fullfill this optical selection criterium. We are not able to draw any conclusions about the number of WTTS fainter than $m_R \simeq 15$ or about sources where only objects fainter than this limit can be found within the error circle. However, there seems to be a limit on the ratio f_X/f_{opt} of X-ray fluxes f_X and optical fluxes f_{opt}, which implies that WTTS fainter than $m_R \simeq 15$ would not be detected by the RASS anyway.

We conclude, that we have identified as yet about 40% (83/203) of the WTTS detected as X-ray sources in the RASS (where the number of 203 is the addition of the 83 WTTS yet discovered and the 120 more WTTS estimated among the yet unidentified RASS sources), and that the WTTS which are RASS sources represent about 31(±0.09)% of all WTTS in Lupus. Thus in total about 650 WTTS should be present in the Lupus SFR, including those already found by us. In contrast, from optical surveys (Thé 1962, Schwartz 1977) only some 48 CTTS are known in this SFR.

Therefore, for the whole area studied, we obtain a WTTS/CTTS ratio of about 13, while for the dark clouds, where the CTTS are concentrated, the ratio is about unity. A similar variation of the WTTS/CTTS ratio has been found for the Taurus SFR (Wichmann et al. 1996a, Neuhäuser et al. 1995a). This large difference is due to the completely different spatial distribution of WTTS and CTTS.

7. Spatial distribution

The hitherto known population of pre-main sequence stars in Lupus, as found by optical surveys, is concentrated in four subgroups (Krautter 1991). One of the main goals of our survey of TTS in the Lupus SFR was to determine the spatial distribution of these stars on a relatively large scale, to see whether this clustering also applies to X-ray selected TTS. The spatial distribution of TTS as found by our work is shown in Fig. 3. TTS found by means of pointed ROSAT observations are not plotted, because these pointed observations are biased spatially. For comparison we show the spatial distribution of the previously known TTS. It is immediately obvious that our sample of X-ray selected TTS in this SFR is spatially distributed over the whole region of interest, in marked contrast to the TTS known prior to ROSAT.

7.1. Statistical tests

Following our paper on a similar survey in the Taurus-Auriga SFR (Wichmann et al. 1996a), we applied two different statistical tests, the nearest-neighbour distance (NND) test (Gomez et al. 1993) and the two-dimensional Kolmogorov-Smirnov (D2KS-) test (Fasano & Franceschini 1987, Press et al. 1992) to our sample of newly dis-

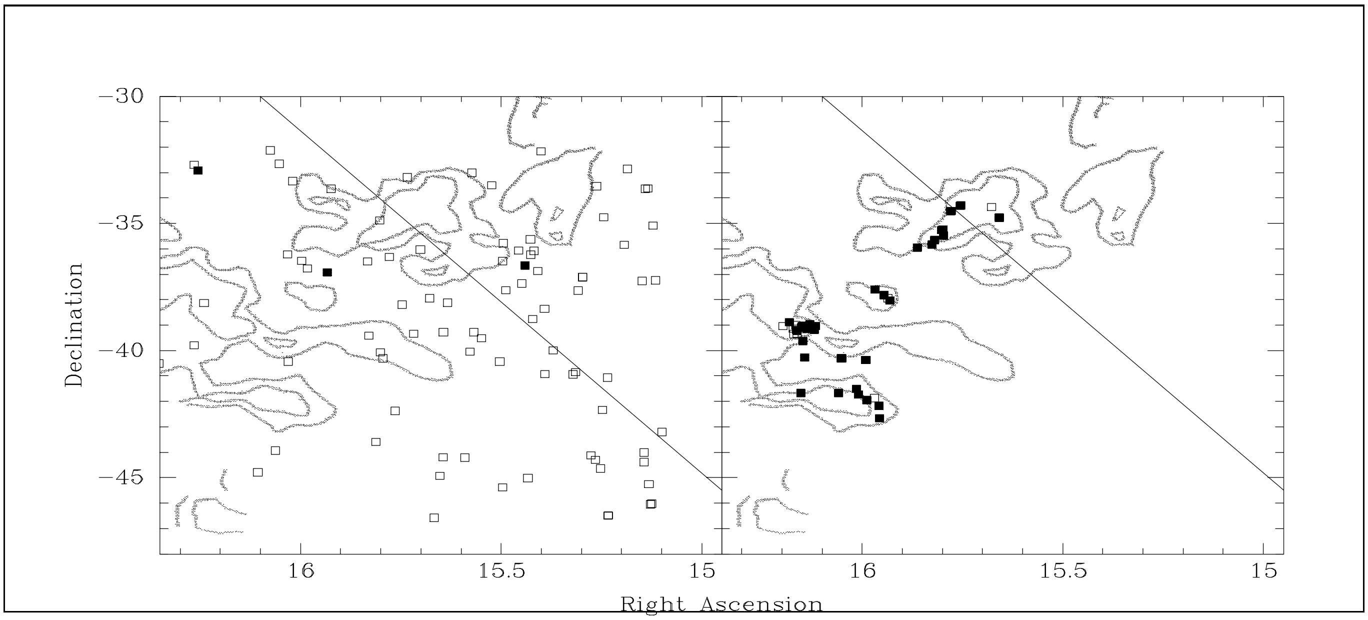

Fig. 3. Spatial distribution of our sample of new RASS-discovered TTS (left panel) and the previously known TTS in the study region (right panel). CTTS are mrked by filled squares, WTTS by open squares. Gould's Belt is shown by the solid line. Also plotted are the two lowest contours of the CO map of Murphy et al. (1986).

covered TTS in order to obtain quantitative information on their spatial distribution and its difference with respect the TTS known prior to ROSAT. As the pointed observations have been carried out in the areas where the previously known TTS are clumped, TTS found by means of these pointed observations are not used for this analysis.

7.1.1. Nearest-neighbour distance test

The distribution of nearest-neighbour distances for the RASS-discovered TTS as well as for the TTS known prior to ROSAT is shown in Fig. 4. As expected, the previously known TTS show strong clustering, with a median NND of $\langle NND \rangle = 0.64$, much lower than the expectation value of $\langle NND_R \rangle = 8.0$, for a uniform random distribution. For the RASS-discovered TTS we obtain $\langle NND \rangle = 3.44$ as compared to the expectation value of $\langle NND_R \rangle = 6.0$.

The significance of the observed excess of small NNDs for the RASS-discovered WTTS can be calculated in the following way: in a given bin, the probability for n or more counts when $\langle n \rangle$ counts are expected, is given by the cumulative Poisson probability $P(\leq n, \langle n \rangle)$. A random sample will yield the observed excess for $\Theta \leq 10'$ with a probability of 8×10^{-6}; for $10' < \Theta \leq 20'$ with a probability of 2×10^{-5}; for $20' < \Theta \leq 30'$ with a probability of 0.248; and for $30' < \Theta \leq 40'$ with a probability of 0.011.

Thus at the smallest NNDs, the observed excess is indeed highly significant. From Fig. 3 it seems that in fact some clumps may be present in the distribution, along with a possible overdensity in the northern part of the study area.

7.1.2. 2D-Kolmogorov-Smirnov test

This conclusion is further strengthened by the result of a two-dimensional Kolmogorov-Smirnov test (for a description see Wichmann et al. 1996a). Comparing the spatial distribution of the RASS-discovered TTS to a model of uniform distribution, the test statistic D has a value of $D = 0.283$, corresponding to a probability P of only $P = 0.0005$ for the hypotheses of a uniform distribution. A closer inspection shows that the most significant dividing point is -40.9^o and 15.3^h, with the quadrant southeast of this point being the most underpopulated with respect to a uniform distribution.

A comparison with Fig. 3 shows that in fact many of the new WTTS seem to be located around Gould's Belt (cf. Gould 1879, Bahcall et al. 1987), while especially the southeastern part of our survey area, i.e. the part most distant from Gould's Belt, seems to show a low surface density of new WTTS. As the galactic plane lies south of our survey region (in Fig. 3, the southeastern edge is at b= 2.1^o, the southwest edge at b=10.6^o) this implies that the spatial distribution of RASS-discovered WTTS in Lupus correlates with Gould's Belt rather than with the galactic plane.

8. Conclusions

Using data from the German X-ray satellite ROSAT, we have studied an area of 230 square degrees of the Lupus SFR in search for new WTTS. On the basis of the ROSAT All-Sky Survey, 86 new WTTS and 3 CTTS could be discovered. 47 more TTS were discovered using pointed

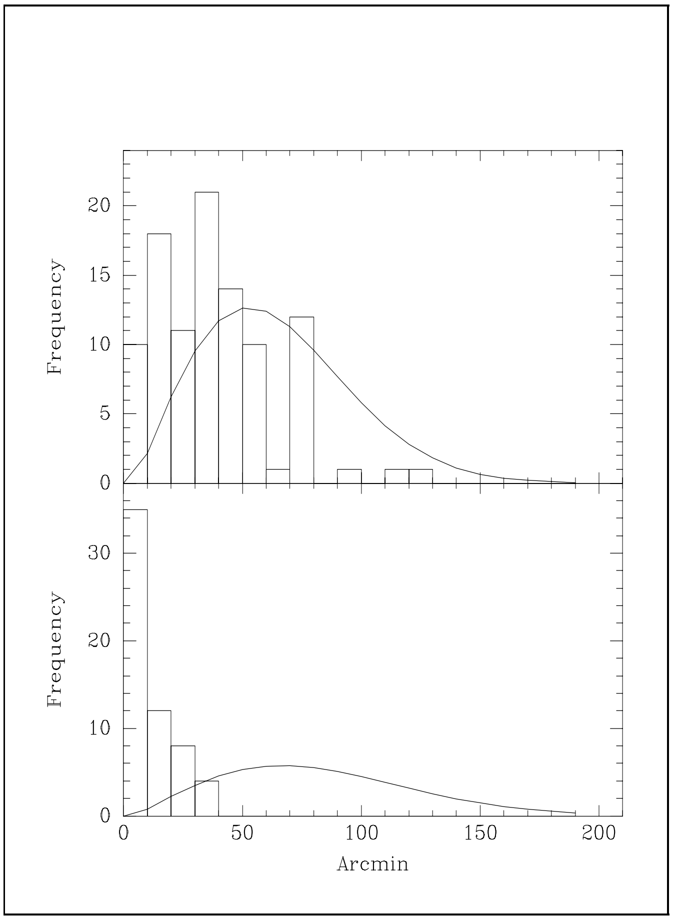

Fig. 4. Distribution of nearest-neighbour distances for previously known TTS (lower panel) and TTS found by the RASS (upper panel). Overplotted are the expected (Poisson) distributions for a random spatial distribution.

ROSAT observations of the Lupus 1–3 clouds. Comparing the XLF of the RASS-discovered WTTS in Lupus with an unbiased XLF for non-X-ray discovered WTTS in Taurus (Neuhäuser et al., 1995b), we were able to estimate the completeness of the RASS to about 31%.

Although, due to its limited sensitivity, only a part of the total population is sampled with the RASS, its spatial completeness allowed us to investigate for the first time the spatial distribution of WTTS in the Lupus SFR on a large scale. We find that the numerous WTTS discovered by us are distributed over the whole area of our survey, contrary to the CTTS in the Lupus SFR, which are found almost exclusively in the vicinity of the dark clouds. Moreover, although our survey covers a large area including and surrounding the known concentrations of PMS stars, from the spatial distribution of our new WTTS we presume that we still do not sample all of the WTTS in the Lupus SFR, as WTTS are found up to the borders of our study region. The somewhat lower surface density of WTTS in the southeastern part of our survey area indicates, that the spatial distribution correlates with Gould's Belt rather than with the galactic plane.

The spatial distribution of the new WTTS discovered by the RASS, especially the observation that many of these stars are found several degrees away from the dense molecular clouds of the Lupus SFR, indicates that these stars might be somewhat older than the hitherto known TTS in Lupus. In this case they could have drifted away from the dark clouds due to a velocity dispersion of 2-3 km/s as measured for TTS in Taurus by Jones & Herbig (1979). We cannot exclude the alternative that these stars were born near their present-day location, and that their parent clouds have dispersed already. Such a model for the formation of widely dispersed TTS in short-lived, rapidly moving cloudlets has recently been proposed by Feigelson (1996). However, this model also predicts that many of the widely dispersed WTTS are older than TTS found in or near dark clouds.

In the Lupus 1–3 dark clouds, with our deep raster scan of pointed observations, numerous new WTTS have been discovered as well. The WTTS/CTTS ratio for the Lupus 1–3 clouds was found to be about unity. However, our work shows that the spatial distribution of WTTS differs significantly from that of the CTTS. Therefore the WTTS/CTTS increases significantly, if a larger area is taken into account. For the whole area of our survey we extrapolate a ratio of about 13, which has to be regarded as lower limit only, because most probably there are more WTTS outside the boundaries of our survey. Similar differences between the distribution of CTTS and WTTS have been found in the Taurus–Auriga SFR as well (Wichmann et al., 1996a. In Taurus–Auriga as well as in Lupus it has been found, that in the most active part of the SFR, near the dark clouds, there is a WTTS/CTTS ratio of about unity, while these parts of the SFR are surrounded by a large, spatially extended population of WTTS.

Acknowledgements. This research was supported by grant KR 1053/3 from the DFG, Germany, grant 50OR90017 (Verbundforschung Astronomie) from the BMFT, Germany, and from CONACyT, Mexico. This research has made use of the SIMBAD database, operated at CDS, Strasbourg, France. R. Wichmann would like to thank the staff at ESO, Chile, for the good support during the observations. The ROSAT project has been supported by the BMFT and the MPG, Germany. Many thanks also to the EXSAS and ROSAT teams at MPE.

Figure 5 shows the spectra of the new TTS in the Hα and Li I region. Finding charts are provided for all new TTS. All charts are 6' × 6'; north is up and east is left.

References

Ambartsumian J.A. 1947, in Stellar Evolution and Astrophysics, Erevan, Acad. Sci. Armen. SSR

Bahcall J.N., Casertano S., Ratnatunga K.U. 1987, ApJ 320, 515

Bouvier J., Cabrit S., Fernandez M., Martin E.L., Matthews J.M. 1993a, AA 272, 176
Bouvier J., Cabrit S., Fernandez M., Martin E.L., Matthews J.M. 1993b, AAS 101, 485
Bouvier et al. 1996, AA submitted
Buscombe W. 1981, MK Spectral Classifications, 5^{th} Ed.
Buscombe W. 1988, MK Spectral Classifications, 7^{th} Ed.
Cruddace R. G., Hasinger G. R., Schmitt J. H. M. M.: 1988, in Astronomy from Large Databases, Murtagh, F. und Heck, A. (eds.), p. 177
Fasano G., Franceschini A. 1987, M.N.R.A.S. 225, 155
Feigelson E.D., 1996, ApJ, in press
Ghez A.M., Neugebauer G., Matthews K. 1993, AJ 106, 2005
Gomez M., Hartmann L., Kenyon S.J., Hewett R. 1993, AJ 105, 1927
Gould B.A., in Uranometria Argentina, P.E. Corni, Buenos Aires, p. 355, 1879
Herbig G.H. 1978, in Problems of Physics and Evolution of the Universe, Erevan, Acad. Sci. Armen. SSR
Hughes J., Hartigan P., Clampitt L. 1993, AJ 104, 680
Hughes J., Hartigan P., Krautter J., Kelemen J. 1994, AJ 108, 1071
Jones B.F., Herbig G.H. 1979, AJ 84, 1872
Krautter J. 1991, in Low Mass Star Formation in Southern Molecular Clouds, ESO Report No. 11, edt. B. Reipurth, p. 127
Leinert C., Zinnecker H., Weitzel N., et al. 1993, AA 278, 129
Motch C., Belloni T., Buckley D., et al. 1991, A&A 246, L24
Murphy D.C., Cohen R., May J. 1986, A&A 167, 234
Neuhäuser R., Sterzik M.F., Schmitt J.H.M.M., Wichmann R. Krautter J. 1995a, A&A 295, L5
Neuhäuser R., Sterzik M.F., Schmitt J.H.M.M., Wichmann R. Krautter J. 1995b, A&A, 297, 391
Paresce F. 1984, AJ 89, 1022
Pfeffermann E., Briel U.G., Hippmann H., et al. 1986, In: Soft X-Ray Optics and Technology, Proc. SPIE, 733, 519
Press W. H., Teukolsky S. A., Vetterling W. T., Flannery B. P. 1992, Numerical Recipes, Cambridge Univ. Press
Raymond J.C., Smith B.S. 1977, ApJSS 35, 419
Schwartz R. D. 1977, ApJSS 35, 161
Stocke J.T., Morris S.L., Gioia I. M., Maccacaro T., Schild R. 1991, ApJSS 76, 813
Thé P.-S. 1962, Contrib. Bosscha Obs., No. 15
Trümper J. 1983, Adv. Space Res. 2, 241
Vrba F.J., Rydgren A.E. 1985, AJ 90, 1490
Wichmann R., Krautter J., Schmitt J.H.M.M., et al. 1996a, AA in press
Wichmann R., Krautter J., Covino E., et al. 1996b, AA submitted

Fig. 5. Low-dispersion spectra of new WTTS in Lupus. Shown is the Hα and Li I region.

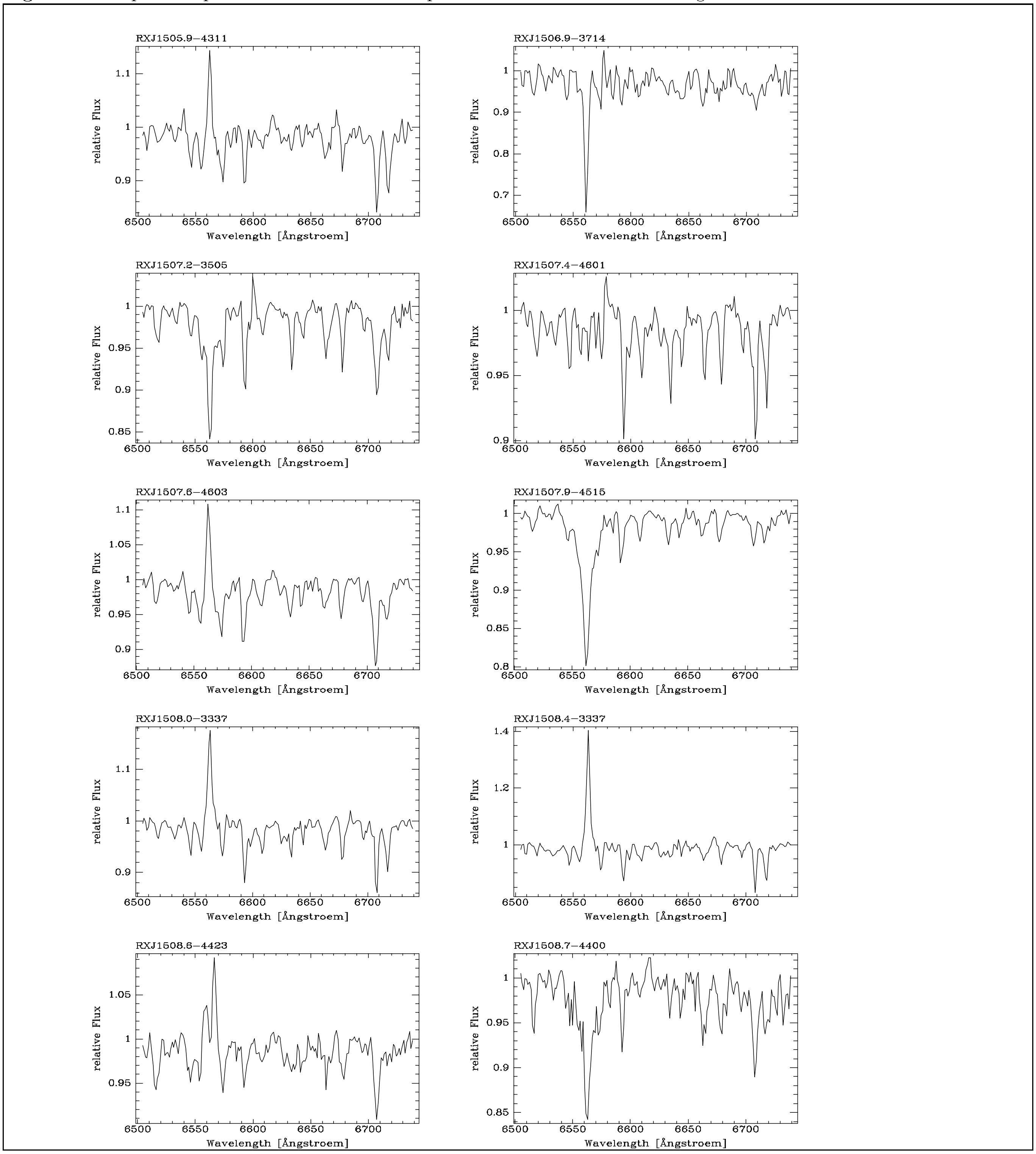

Fig. 5. (cont.)

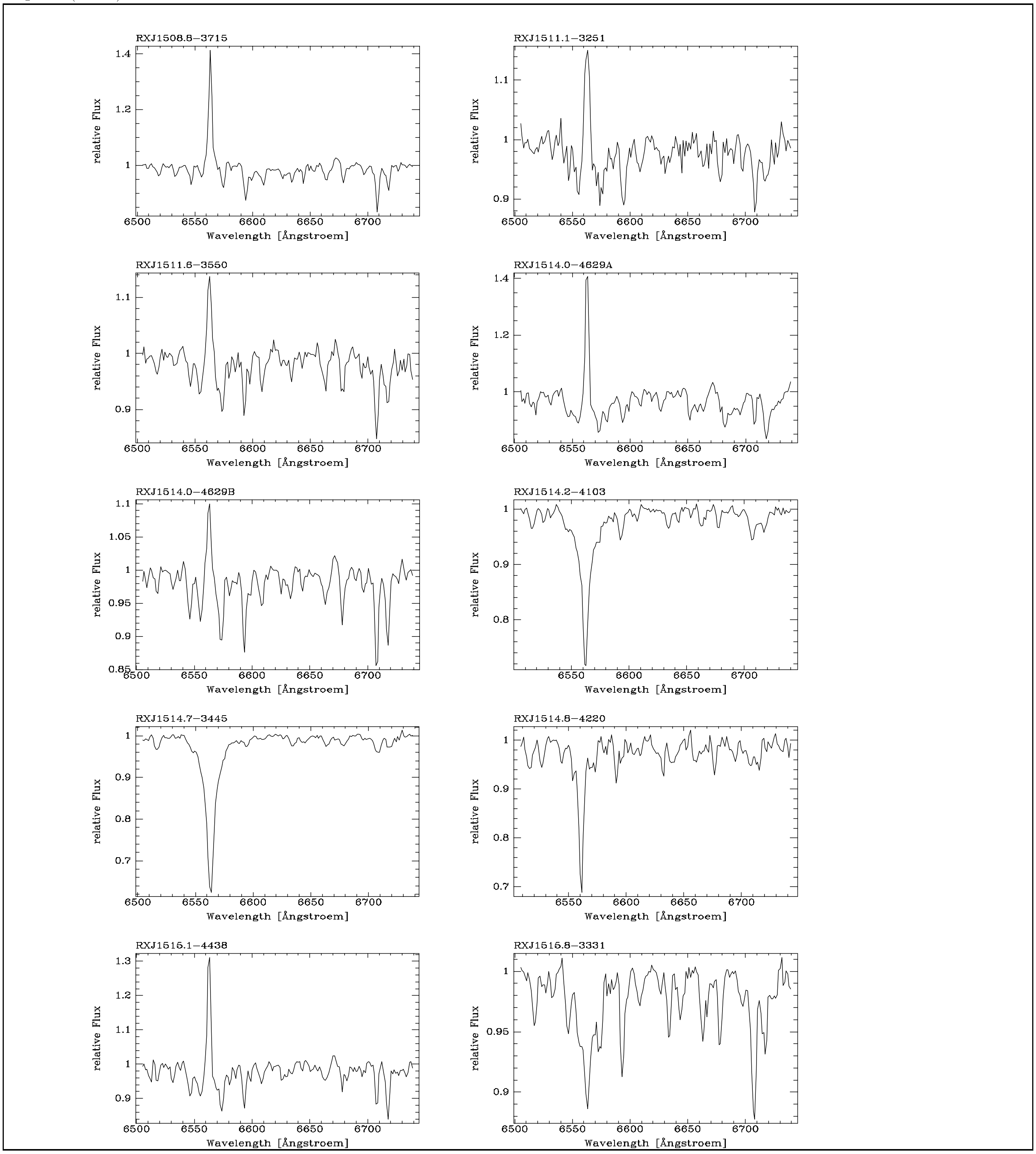
RXJ1508.8−3715
RXJ1511.1−3251
RXJ1511.6−3550
RXJ1514.0−4629A
RXJ1514.0−4629B
RXJ1514.2−4103
RXJ1514.7−3445
RXJ1514.8−4220
RXJ1515.1−4438
RXJ1515.8−3331
relative Flux
Wavelength [Ångstroem]

Fig. 5. (cont.)

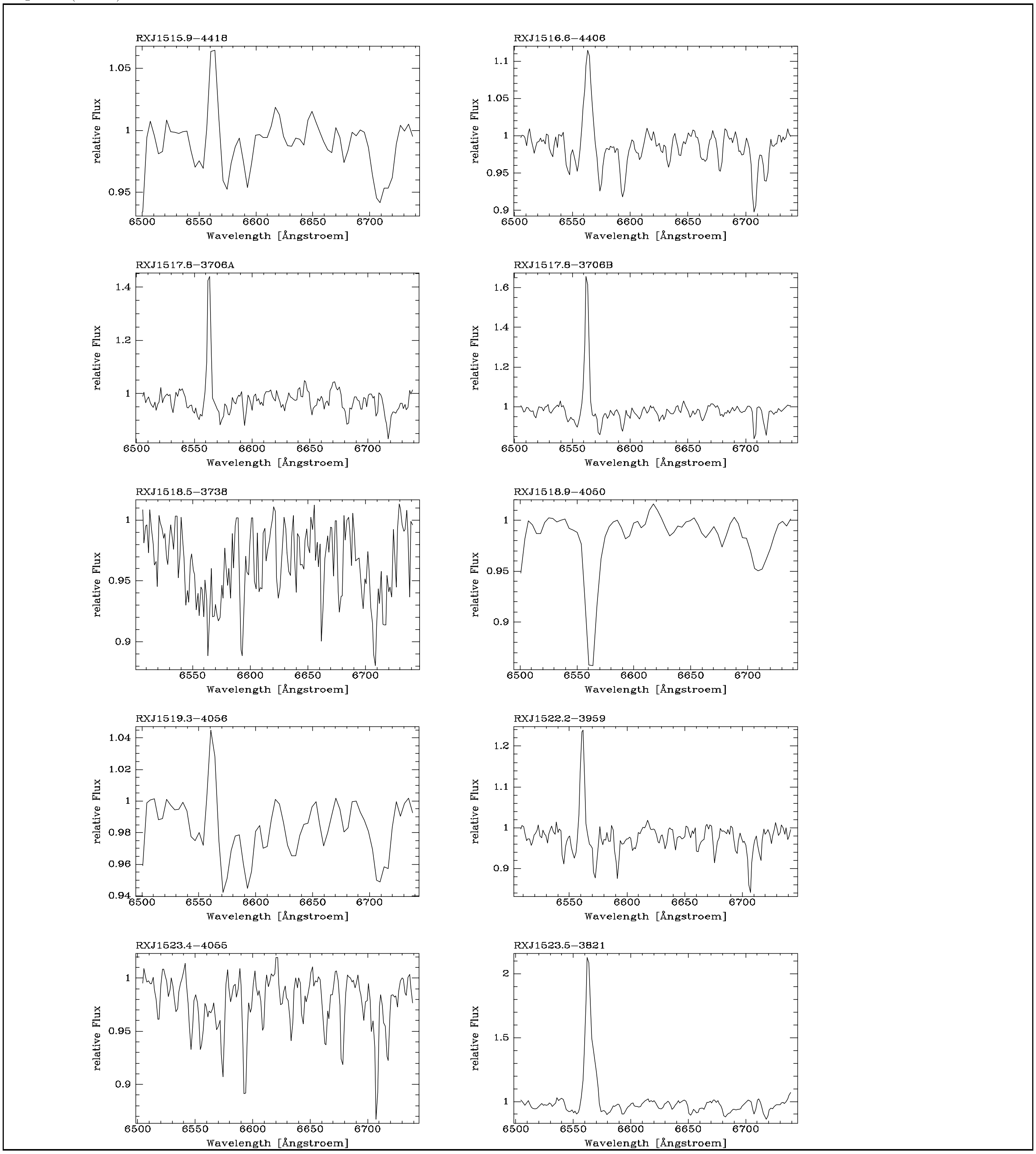
RXJ1515.9−4418
RXJ1516.6−4406
RXJ1517.8−3706A
RXJ1517.8−3706B
RXJ1518.5−3738
RXJ1518.9−4050
RXJ1519.3−4056
RXJ1522.2−3959
RXJ1523.4−4055
RXJ1523.5−3821
relative Flux
Wavelength [Ångstroem]

Fig. 5. (cont.)

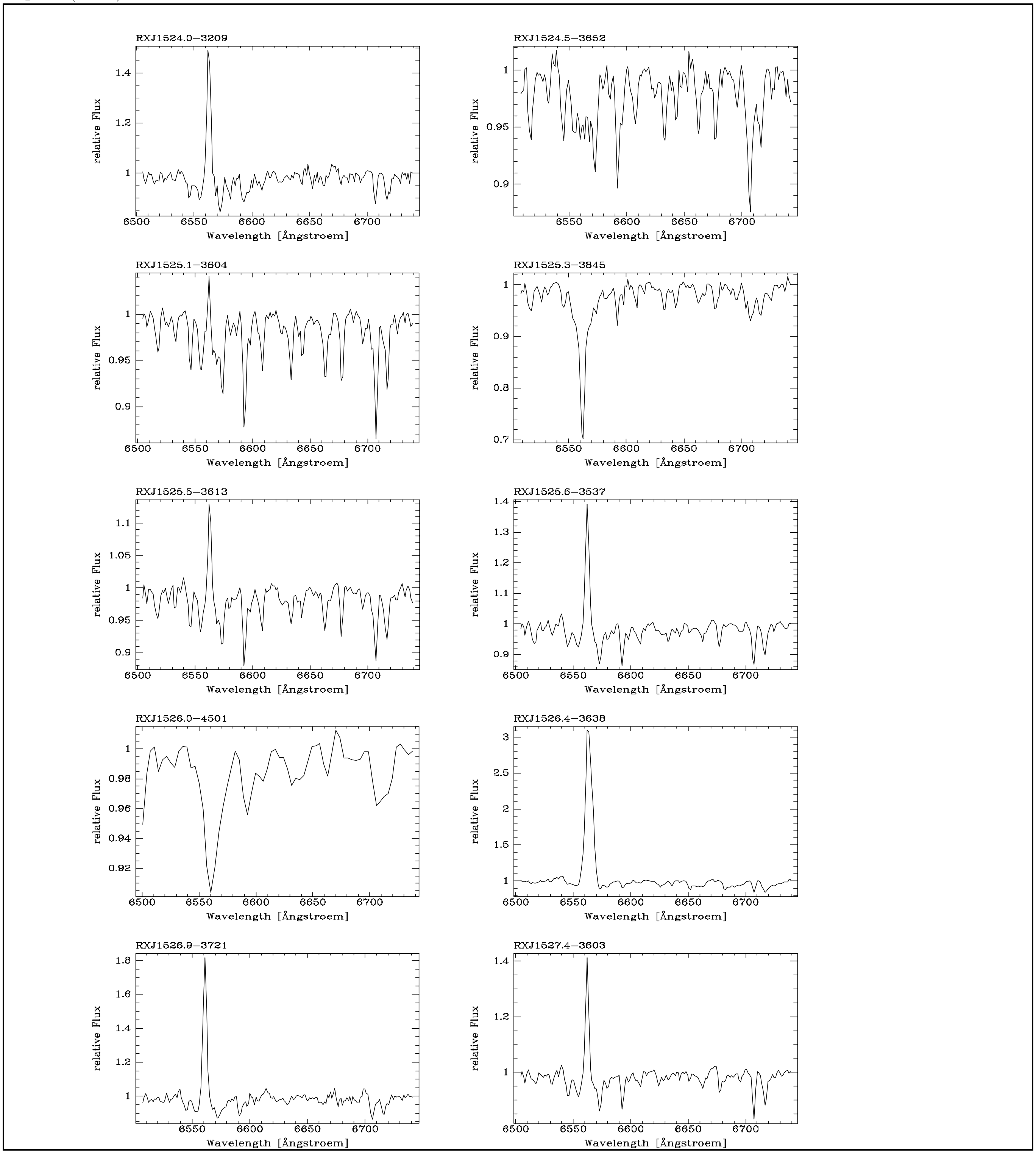
RXJ1524.0−3209
RXJ1524.5−3652
RXJ1525.1−3604
RXJ1525.3−3845
RXJ1525.5−3613
RXJ1525.6−3537
RXJ1526.0−4501
RXJ1526.4−3638
RXJ1526.9−3721
RXJ1527.4−3603
relative Flux
Wavelength [Ångstroem]

Fig. 5. (cont.)

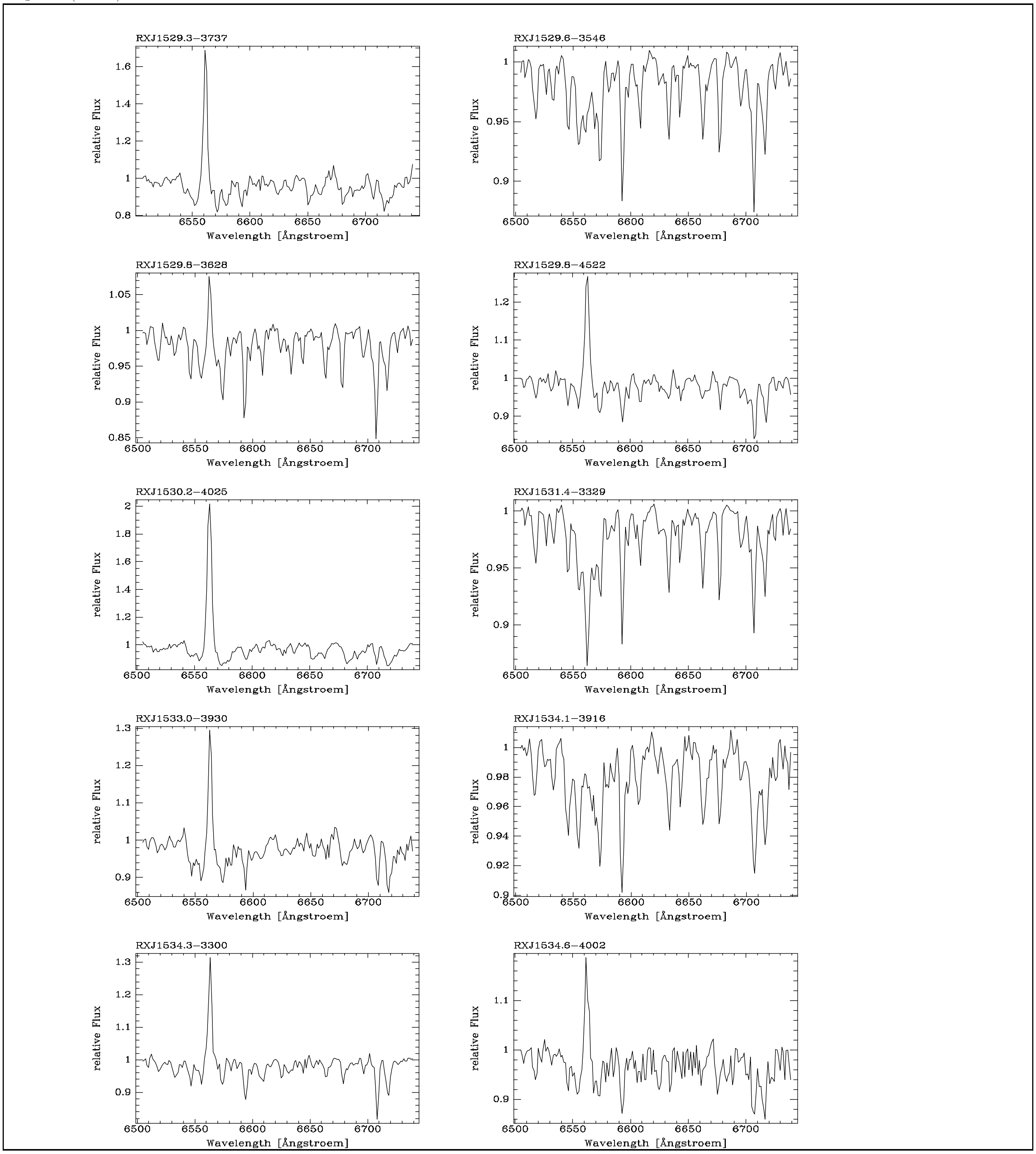
RXJ1529.3–3737
RXJ1529.6–3546
RXJ1529.8–3628
RXJ1529.8–4522
RXJ1530.2–4025
RXJ1531.4–3329
RXJ1533.0–3930
RXJ1534.1–3916
RXJ1534.3–3300
RXJ1534.6–4002
relative Flux
Wavelength [Ångstroem]

Fig. 5. (cont.)

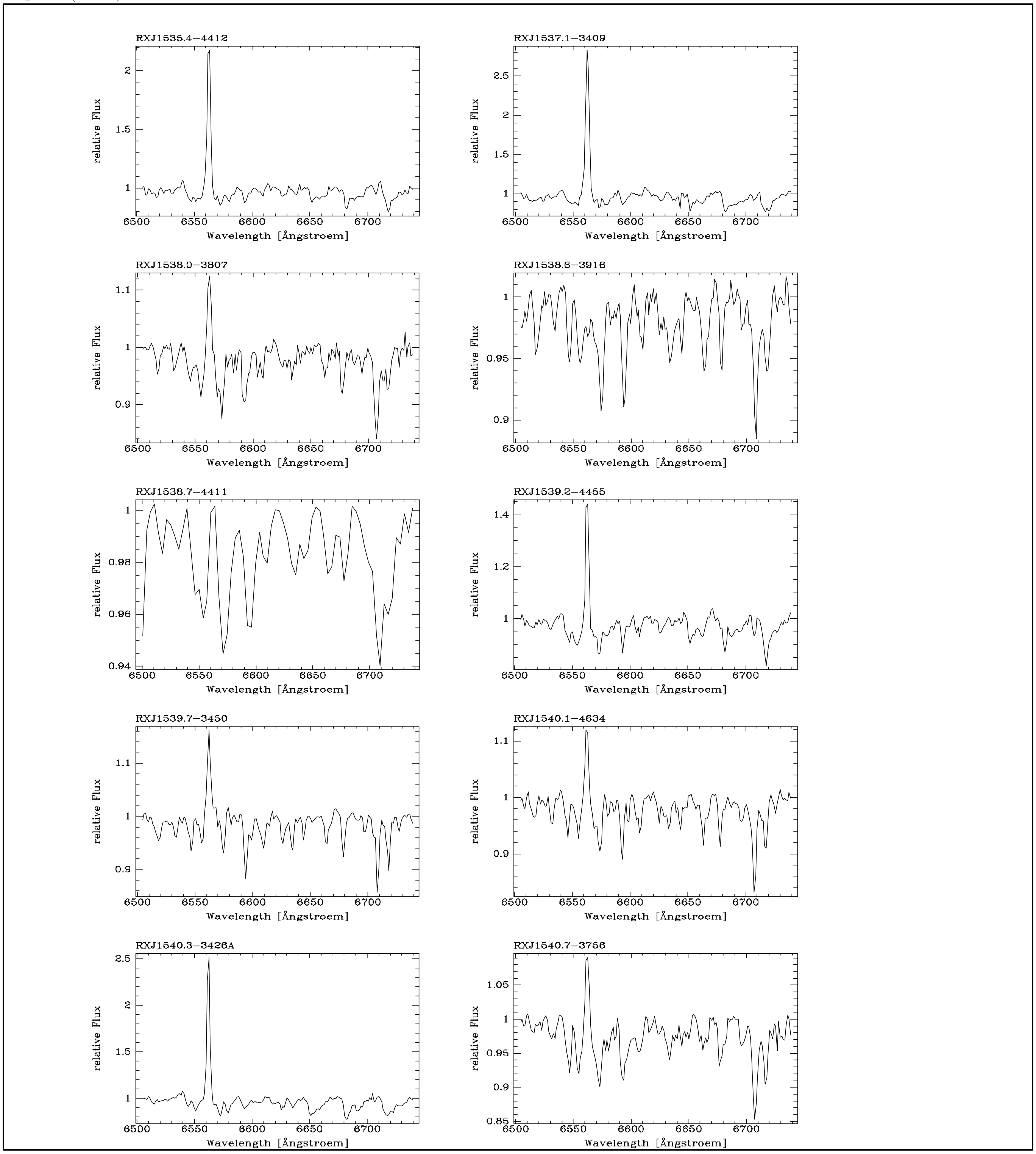
RXJ1535.4−4412
RXJ1537.1−3409
RXJ1538.0−3807
RXJ1538.6−3916
RXJ1538.7−4411
RXJ1539.2−4455
RXJ1539.7−3450
RXJ1540.1−4634
RXJ1540.3−3426A
RXJ1540.7−3756
relative Flux
Wavelength [Ångstroem]

Fig. 5. (cont.)

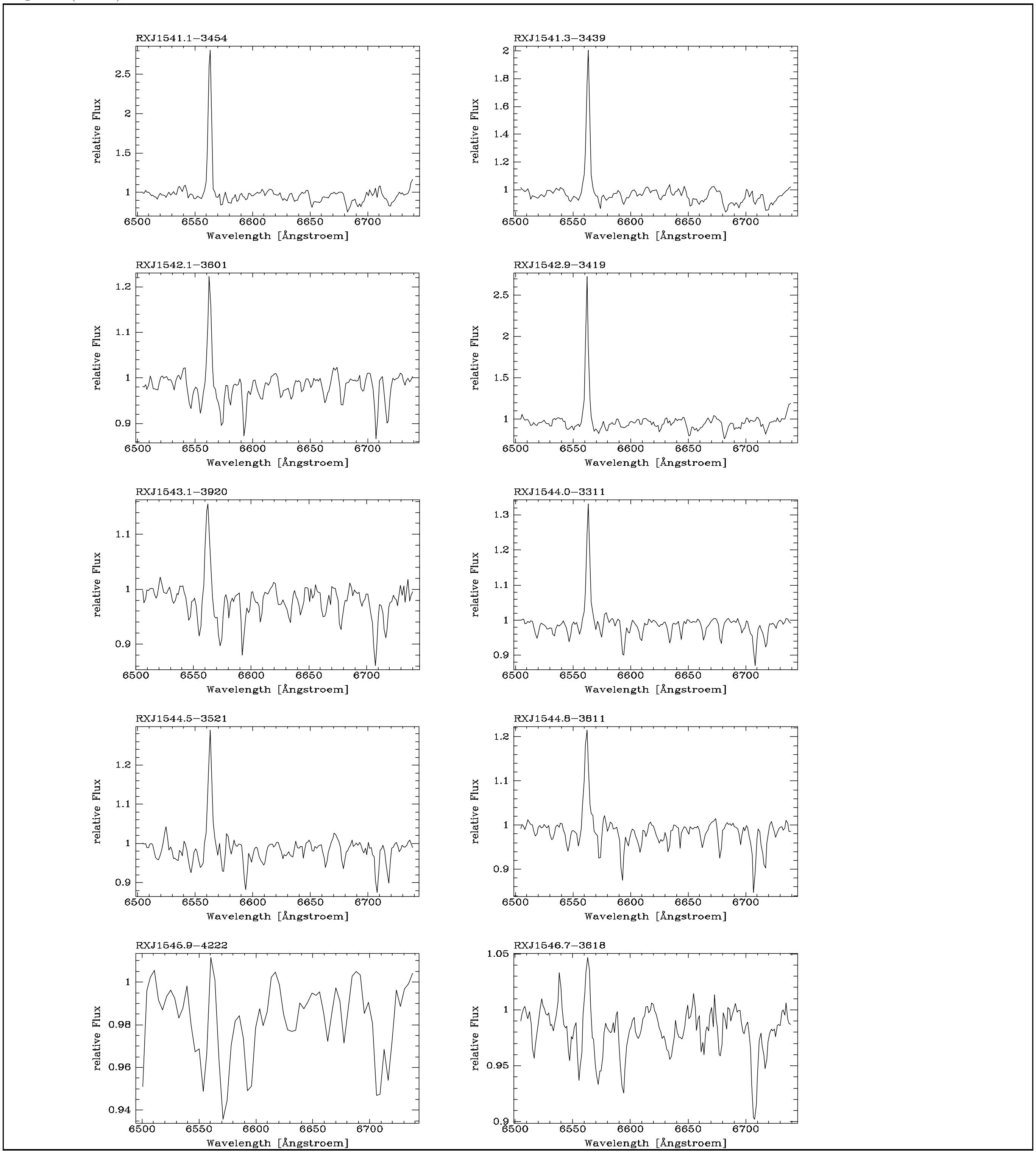
RXJ1541.1−3454
RXJ1541.3−3439
RXJ1542.1−3601
RXJ1542.9−3419
RXJ1543.1−3920
RXJ1544.0−3311
RXJ1544.5−3521
RXJ1544.6−3811
RXJ1545.9−4222
RXJ1546.7−3618
relative Flux
Wavelength [Ångstroem]

Fig. 5. (cont.)

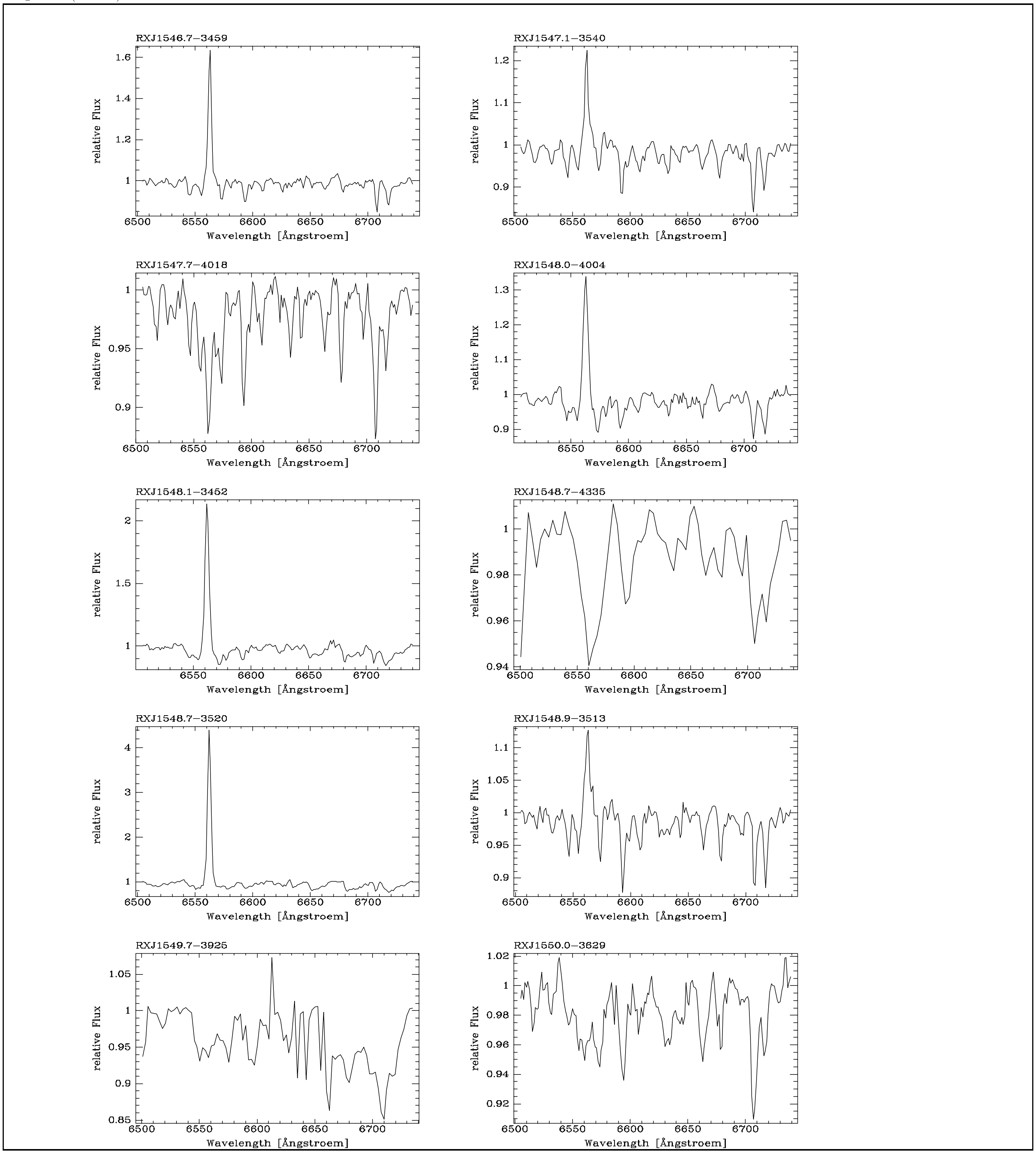
RXJ1546.7−3459
RXJ1547.1−3540
RXJ1547.7−4018
RXJ1548.0−4004
RXJ1548.1−3452
RXJ1548.7−4335
RXJ1548.7−3520
RXJ1548.9−3513
RXJ1549.7−3925
RXJ1550.0−3629
relative Flux
Wavelength [Ångstroem]

Fig. 5. (cont.)

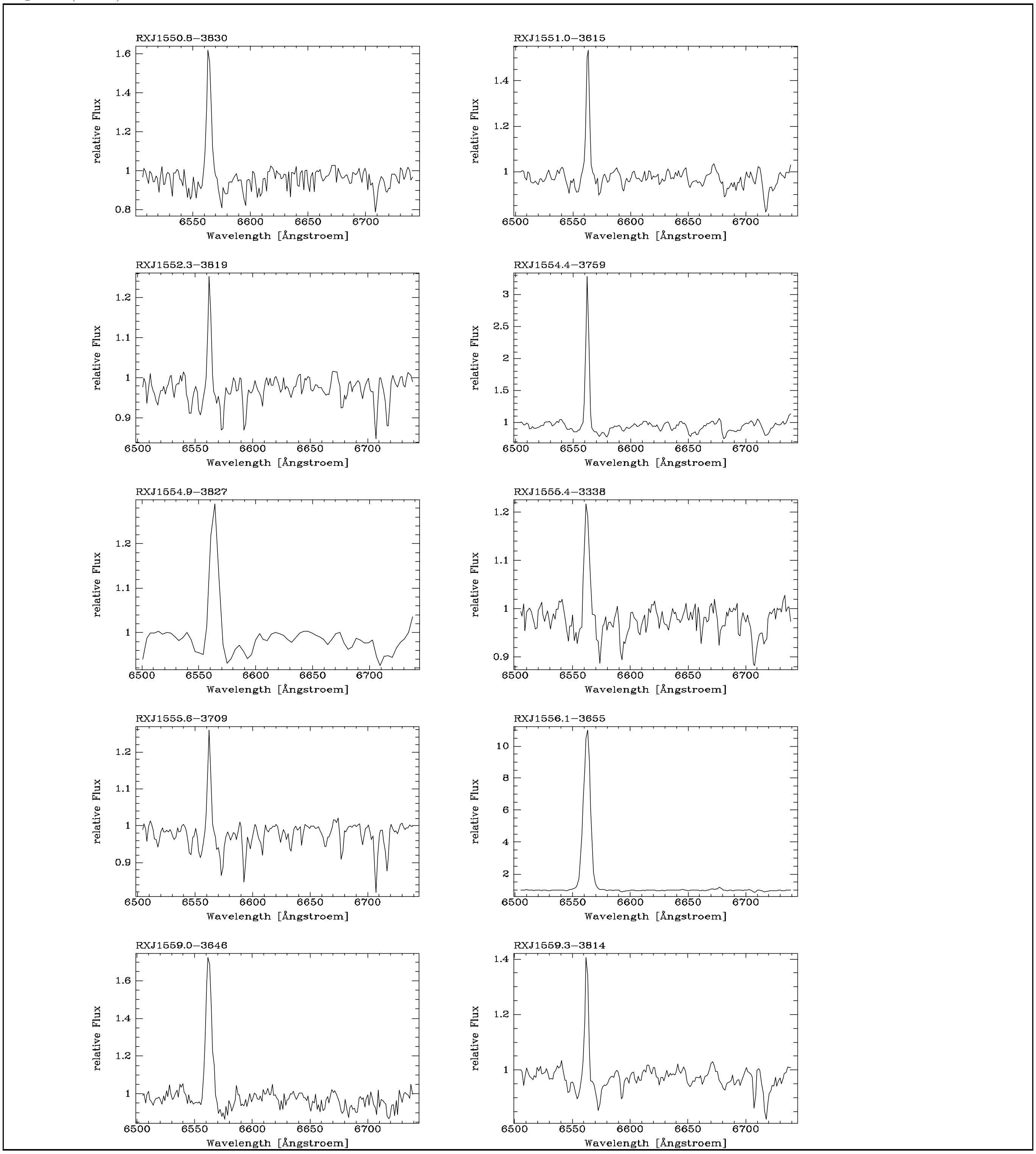
RXJ1550.8−3830
RXJ1551.0−3615
RXJ1552.3−3819
RXJ1554.4−3759
RXJ1554.9−3827
RXJ1555.4−3338
RXJ1555.6−3709
RXJ1556.1−3655
RXJ1559.0−3646
RXJ1559.3−3814
relative Flux
Wavelength [Ångstroem]

Fig. 5. (cont.)

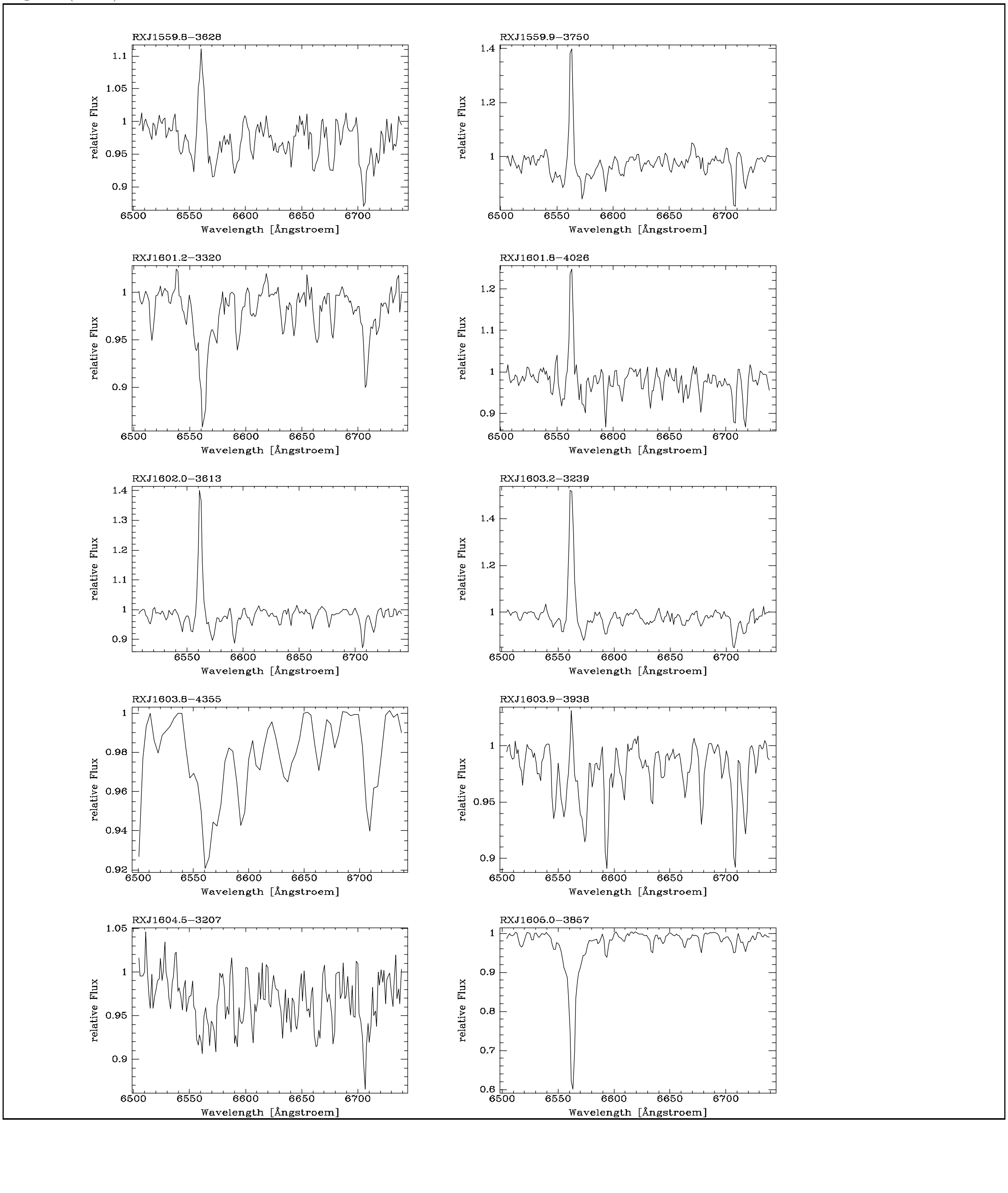
RXJ1559.8−3628
RXJ1559.9−3750
RXJ1601.2−3320
RXJ1601.8−4026
RXJ1602.0−3613
RXJ1603.2−3239
RXJ1603.8−4355
RXJ1603.9−3938
RXJ1604.5−3207
RXJ1605.0−3857
relative Flux
Wavelength [Ångstroem]

Fig. 5. (cont.)

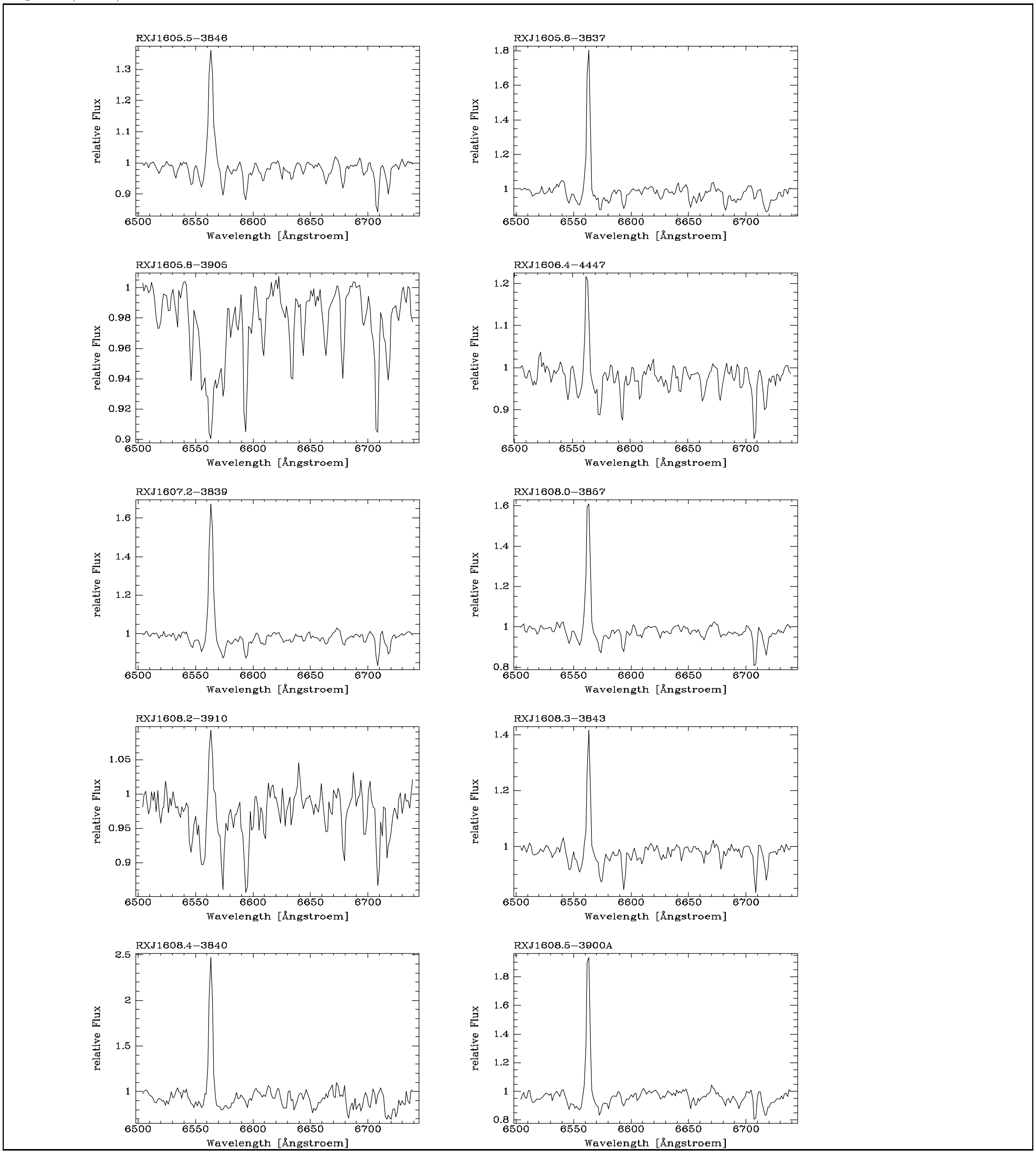
RXJ1605.5−3846
RXJ1605.6−3837
RXJ1605.8−3905
RXJ1606.4−4447
RXJ1607.2−3839
RXJ1608.0−3857
RXJ1608.2−3910
RXJ1608.3−3843
RXJ1608.4−3840
RXJ1608.5−3900A
relative Flux
Wavelength [Ångstroem]

Fig. 5. (cont.)

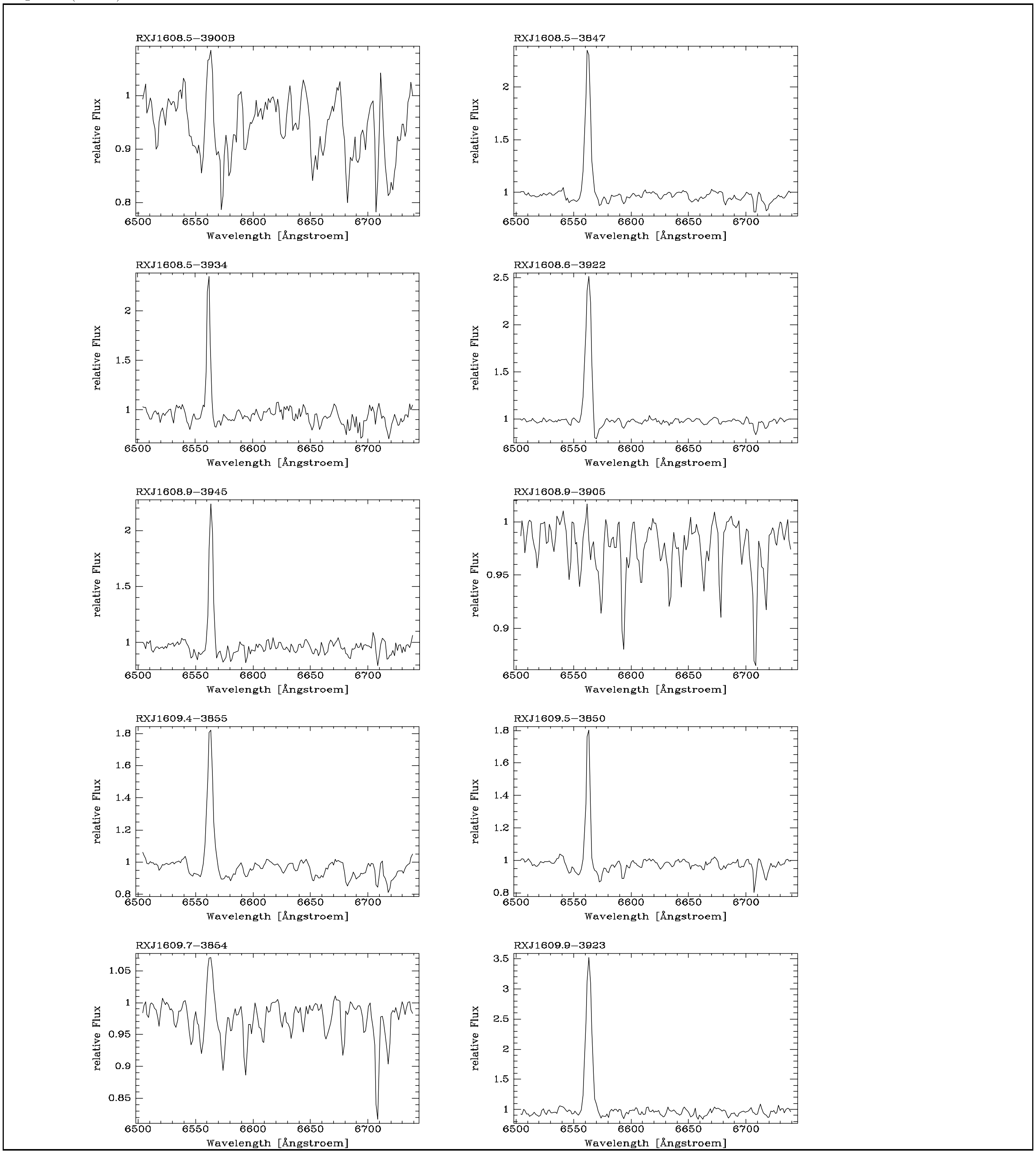
RXJ1608.5−3900B
RXJ1608.5−3847
RXJ1608.5−3934
RXJ1608.6−3922
RXJ1608.9−3945
RXJ1608.9−3905
RXJ1609.4−3855
RXJ1609.5−3850
RXJ1609.7−3854
RXJ1609.9−3923
relative Flux
Wavelength [Ångstroem]

Fig. 5. (cont.)

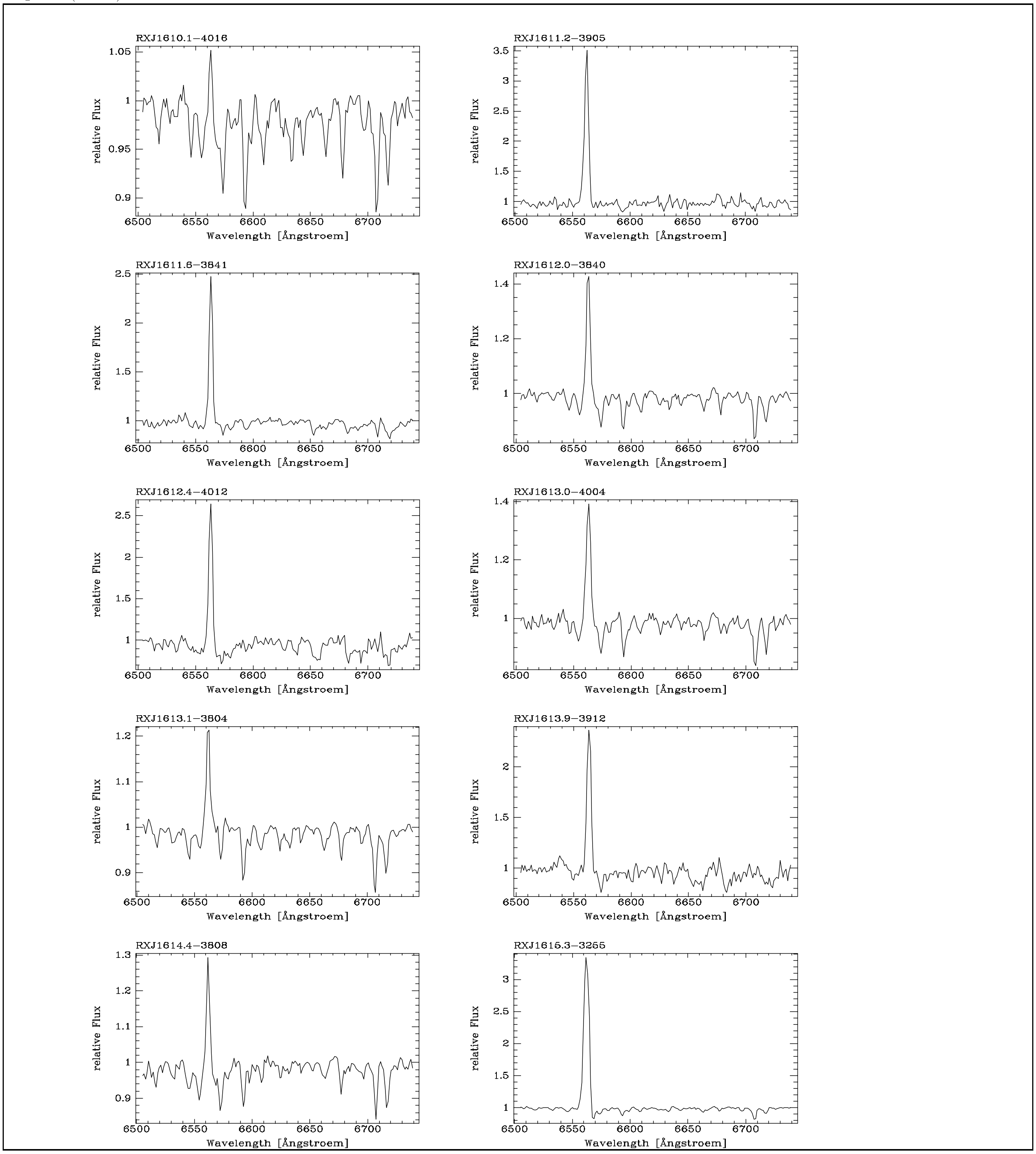
RXJ1610.1–4016
RXJ1611.2–3905
RXJ1611.6–3841
RXJ1612.0–3840
RXJ1612.4–4012
RXJ1613.0–4004
RXJ1613.1–3804
RXJ1613.9–3912
RXJ1614.4–3808
RXJ1615.3–3255
relative Flux
Wavelength [Ångstroem]

This article was processed by the author using Springer-Verlag
LaTeX A&A style file *L-AA* version 3.

Fig. 5. (cont.)

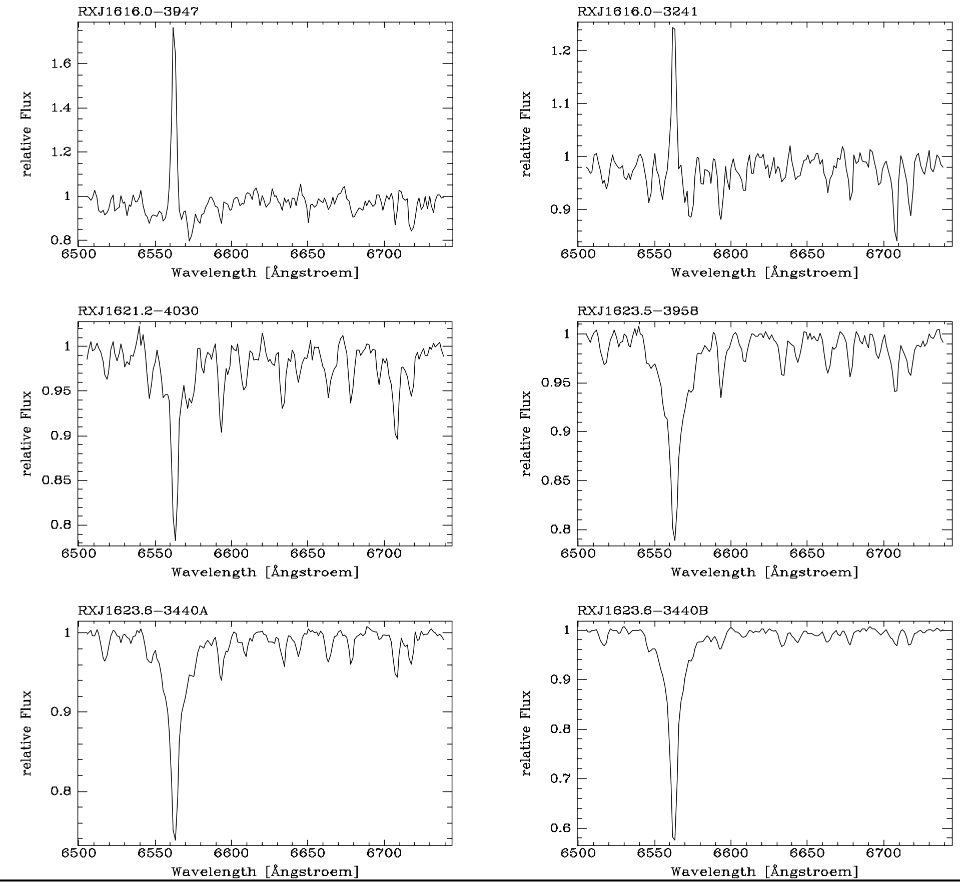
RXJ1616.0−3947
RXJ1616.0−3241
RXJ1621.2−4030
RXJ1623.5−3958
RXJ1623.6−3440A
RXJ1623.6−3440B
relative Flux
Wavelength [Ångstroem]